Research Square

Preprints are preliminary reports that have not undergone peer review.
They should not be considered conclusive, used to inform clinical practice,
or referenced by the media as validated information.

Spatial-temporal evolution and multidimensional gradient differentiation of production-living-ecological spaces in Yanhe River Basin, China

xue Zhou
Guizhou University
Haotian Wu
Guizhou University
Zhi Cao
caoz@igsnrr.ac.cn

Institute of Geographic Sciences and Natural Resources Research

Research Article

Keywords: Production–Living–Ecological Spaces, Socio–economic gradients, Functional value, Spatial–temporal evolution, Yanhe River Basin

Posted Date: November 6th, 2026

DOI: https://doi.org/10.21203/rs.3.rs-10688366/v1

License: This work is licensed under a Creative Commons Attribution 4.0 International License.
Read Full License

Additional Declarations: No competing interests reported.

Abstract

Quantifying multi–dimensional gradient differentiation of production–living–ecological spaces (PLEs) is essential for guiding differentiated spatial planning in ecologically fragile regions. However, existing studies rarely examine PLE functional value variation across both intensity zones and coupled natural–socio–economic gradients at the grid scale. Taking the Yanhe River Basin as the study area, this study constructed a grid–scale PLE functional value evaluation system to analyze PLE spatiotemporal evolution and gradient differentiation along six natural and socio–economic dimensions from 2000 to 2025. The results showed that: (1) All three spatial functions exhibited significant growth and convergence toward high–value zones, with PS high–value zone expanding from 44.9% to 53.0% and ES high–value zone from 55.8% to 67.3%, while LS high–value zones remained concentrated along the Yanhe River main course. (2) Natural gradients exerted a dominant organizing effect on PLE distribution, with the most dramatic transformations in flat terrain (< 3°), low elevations (< 945 m), and river–remote zones (> 1200 m), whereas ES improvements were most pronounced in steep terrain (> 25°), indicating that ecological restoration effectively targeted topographically constrained areas. (3) Road network expansion was the primary socio–economic driver of PLE restructuring, with the most substantial ES gains (+ 8.9%) in road–remote zones (> 6000 m), while the highest population density zone exhibited a trade–off of PS and LS gains against sharp ES decline. These findings underscore the necessity of incorporating multi–dimensional gradient analysis into territorial spatial planning to formulate differentiated strategies balancing ecological restoration and sustainable development in the Loess Hilly–Gully region.

1 Introduction

Territorial space, a complex geosystem, serves as the objective carrier of territorial functions within the human–earth system (Bondarenko et al., 2019; Hu et al, 2022). Globally, land use change has been the primary driver of terrestrial ecosystem transformation, posing unprecedented challenges to food security, biodiversity conservation, and climate resilience (Winkler et al., 2021; Trindade Rodrigues et al., 2026). Against this backdrop, production–living–ecological spaces (PLEs), comprising production space (PS), living space (LS) and ecological space (ES), have emerged as a coherent framework for analyzing spatial conflicts and functional trade–offs in multifunctional territorial systems (Verburg et al., 2009; Liu et al., 2017; Ji et al., 2023). The PLEs concept has gained particular prominence in China, which formally established a national territorial spatial planning system in 2012, with the strategic objective of intensive and efficient PS, moderately scaled LS, and beautiful ES (Gao et al., 2025). Optimizing the configuration of production, living, and ecological spaces has thus become a critical aspect of spatial planning, so as to achieving sustainable development in China (Lin et al., 2022; Liu et al., 2025).

The spatial patterns and layout of PLEs are co–determined by environmental variables and anthropogenic influences, resulting in specific territorial functions. Natural factors, such as the physiographic environment, contribute to spatial heterogeneity in climate, soil types, and vegetation cover (Philpott et al., 2008; Liao, 2022). This is particularly evident in hilly and mountainous regions,

where the spatial layout of territorial space is strongly influenced by elevation, slope gradient, and slope aspect (Yu et al., 2020; Valdivia–Orrego et al., 2024). In contrast to natural factors, socio–economic drivers, intensified by the ongoing global urbanization process, have increasingly reshaped territorial space by altering the functional attributes of PLEs. These anthropogenic forces have gradually become the dominant determinants of PLE spatial patterns (Chen and Zhu, 2022; Uhodnikova et al., 2024). Existing studies have primarily focused on the driving mechanisms of natural and socio–economic factors in shaping territorial spatial differentiation, particularly in river basins and mountainous terrains (Li, 2021; Tao et al., 2022; Liu et al., 2025). However, relatively limited attention has been paid to the coupled natural–socio–economic gradient model to reveal their interactive effects on land functions.

The Yanhe River basin has become one of the areas in the Yellow River basin with the fastest vegetation recovery, with vegetation coverage increasing from 30% to 60% during the past twenty years (Gu et al., 2019; Schmitz et al., 2026). Concurrently, the process of urbanization has led to notable improvements in public welfare, housing infrastructure, and living standards in both urban and rural communities (Gao et al., 2025). Integrating both natural and socio–economic gradients provides a practical framework for examining changes in PLEs. This study supports evidence–based policymaking in the Yanhe River Basin, particularly for optimizing the proportional structure and spatial allocation of production space, living space, and ecological space.

Previous studies have focused more on the process of total area changes in PLEs, especially revealing changes in its landscape patterns, neglecting the spatiotemporal evolution of their internal functional value and multidimensional gradient differentiation. Quantifying the area coverage and functional value of production–living–ecological spaces (PLEs) is essential for identifying areas with the greatest potential for improvement and determining appropriate intervention strategies for sustainable land use. This study aims to investigate the internal functional value and multi–dimensional gradient differentiation of PLEs within the Yanhe River Basin, located in the ecologically fragile Loess hilly–gully region. The innovations and contributions of this study include three aspects. First, this study conducted an in–depth analysis of the quantitative changes in PLEs across diverse functional value zones (high–value zone, moderate–value zone and low–value zone) over the past 20 years. Second, by integrating both natural and socio–economic gradient analysis, this study provides a comprehensive and systematic understanding of the quantitative evolution and spatial differentiation of PLEs. Third, the findings yield valuable policy implications for formulating differentiated spatial layouts and targeted strategies for the allocation of PLEs in ecologically vulnerable and underdeveloped regions with similar environmental and geomorphological characteristics. The remainder of this paper is organized as follows: Section 2, Methodology and Data Sources, introduces the study area and details the study methodology, including the construction of the evaluation index system and the classification of multidimensional gradients. Section 3, Results, presents the findings of this study, focusing on the spatio–temporal distribution characteristics of PLE functions and the patterns of multi–dimensional gradient differentiation. Section 4, Discussion, offers an in–depth interpretation of the PLE results and the broader implications. Section 5, Conclusions, summarizes the key findings and outlines the main conclusions of this study.

2 Materials and Methods

2.1 Study area

Yanhe River Basin is located in the central part of Loess Plateau in Shaanxi Province, China (108°45' – 110°28'E, 36°23–37°17'N), encompassing an area of approximately 7,725 km2. The topography exhibits an elevation gradient rising from southeast to northwest (Fig. 1). Yanhe River Basin is characterized by complex geographical environment with gully density ranging from 2.1 to 4.6 km/km2. It is a temperate continental semi–arid monsoon climate with a mean annual temperature of 9°C and an average annual rainfall of 507 mm. Precipitation is markedly seasonal, with approximately 75% of annual rainfall occurring between July and September. The dominant soil type is yellow loamy soil, noted for its deep, loose structure and high potassium content, which has important implications for land productivity and erosion potential. The Yanhe River Basin, with a total length of 286.9 km, traverses primarily through Ansai District, Baota District, and Yanchang County. The total population in this basin is 685,000, including 417,400 urban population and 267,600 rural population in the year of 2020. Due to its fragile ecological conditions and prolonged anthropogenic disturbances, the basin has experienced severe soil erosion and water loss. Since the large–scale implementation of the 'Green for Grain Program' in 1999, Yanhe River Basin has become one of the most representative area for vegetation coverage on the Loess Plateau, growing from blew 30% to more than 60% (Zhao et al., 2015).

2.2 Data sources and processing

The data used in this study included the followings. Land use maps in 2000 and 2025 with a spatial resolution of 30 m were derived from Resource and Environment Science and Data Center (https://www.resdc.cn/). The first–class land use type adopted in this study included forest, grassland, arable land, construction land, water body and unused land. There were eleven second–class land use types in this study. Digital Elevation Model (DEM) with 7–m resolution was developed from google earth, which was used to derive topographic attributes of elevation and slope. We downloaded China's gridded population counts at a resolution of 3 arcsec (~ 100 m at Equator) free of charge in WorldPop website (https://www.worldpop.org/). Road data in 2020 was collected from Openstreet map (http://www.openstreetmap.org/). The vector road network in the Yanhe River basin in 2005 was extracted from National Fundamental Geo–information Database at the scale of 1:10,0000 (http://www.geodata.cn/index.html). Nighttime lights imageries with the cell size of 1 km × 1 km from 2000 to 2025 were sourced from https://dataverse.harvard.edu/dataset.xhtml?persistentId=doi:10.7910/DVN/GIYGJU (Wu et al., 2022). The identification of PLEs and classification of natural and socio–economic gradient indicators were mainly processed by the raster calculator tool, surface tool, reclassify tools on the ArcGIS 10.2 platform.

2.3 Methods

2.3.1 Quantitative method of PLEs

Land use objectively represents the intensity of economic activities in a certain region and the degree of cumulative effect on the natural ecological environment (Cai, 2001). Land use is characterized by multi–functional characteristics (Wiggering et al., 2006), which integrates provisioning services for socio–economic demands, as well as ecological maintenance capacities and natural regulatory mechanisms (Verburg et al., 2009; Fu et al., 2022). A critical aspect of quantifying PLEs lies in elucidating the multi–functional value of land use from the perspective of human–environment system coupling, which requires the integration of multidisciplinary knowledge (Groot, 2006). Based on the classification system of land use (GBT 21010–2017) and previous studies (Zhang et al., 2025), we constructed a land use classification system for PLEs as shown in Table 2. In this evaluation system, land use types were accessed using a scoring system, where weights ranging from 0 to 5 were assigned based on the relative intensity of land input and output. The functional value of PLEs were calculated at the grid scale according to the land use type systems in Table 1. Subsequently, the natural breakpoint method was applied to classify PLEs' functional value into three categories: low–value zone (scores 0–1), moderate–value zone (scores 1–3), and high–value zone (scores 3–5).

Table 1
Evaluation index system of functional value for PLEs

Land use types	Functional value of PS	Functional value of LS	Functional value of ES
Urban built–up land	5	5	0
Rural settlement	3	3	0
Other construction land	5	0	0
Arable land	3	0	3
Woodland	1	0	5
Grassland	5	0	5
Drainage condition	1	0	1
River canal	0	0	5
Reservoir pond	1	0	1
Beach land	0	0	5
Unused land	0	0	1

2.3.2 The division of multidimensional gradients

Quantifying the gradient differentiation of PLEs will be helpful for in–depth understanding of human–earth interactions and constructing sustainable land use strategies (Schmitz et al., 2012; Ullah et al., 2019). Following the principles of being scientific, representative and comparability, we selected the two

groups of indicators to describe the comprehensive gradients of PLEs, including natural characteristics and socio–economic environment (Fu et al., 2022), as shown in Fig. 2.

The spatial configuration and functional dynamics of PLEs are fundamentally influenced by natural characteristics, including slope, elevation and water capacity. As intrinsic topographic parameters, slope and elevation serve as essential indicators for characterizing terrain complexity, with extensive applications in gradient differentiation analyses across geographical studies (Li et al., 2025; Fu et al., 2026). Especially in mountainous areas like Loess hilly –gully regions, topographical factors are crucial to the spatial layout and functional value of the PLEs (Cao et al., 2024). Furthermore, water capacity in the mountainous areas shows significant spatio–temporal heterogeneity, a phenomenon attributable to the synergistic effects of intricate terrain configurations and regional microclimate variations (Chaif et al., 2025).

The socio–economic conditions of PLEs were determined by population density, nighttime light intensity and road accessibility. Specifically, the population density and nighttime light intensity were adopted to reflect the intensity of anthropogenic activity and the economic pressures on ecosystems (Levin et al., 2020; Li et al., 2024). Road accessibility was employed to characterize spatial connectivity thresholds, serving as a critical indicator of regional infrastructure development levels (Liu et al., 2019). Combining the distribution characteristics of the indicators and previous studies (Wondie et al., 2012; Liu et al., 2017), six indicators were categorized into five classes using quantitative methods (Table 2). Also, we calculated the area coverage and mean functional value of PLEs in different classes.

Table 2
Classification standards of natural and socio–economic gradients

Type	Gradientindicators	Classification				
		□	□	□	□	□
Natural gradients	Slope	<3°	3°–8°	8°–15°	15°–25°	>25°
	Altitude	<945m	945–1100m	1100–1260m	1260–1414m	>1414m
	Distance from the nearest river	<200m	200–500m	500–800m	800–1200m	>1200m
Socio–economic gradients	Population density	>22	3–22	1.6–3	1.3–1.6	<1.3
	Nighttime lights density	>20	10–20	6–10	3–6	<3
	Road accessibility	<500m	500–1500m	1500–3500m	3500–6000m	>6000m

3 Results

3.1 The quantitative characteristics and spatial distribution of PLEs

The results of quantitative characteristics and spatial distribution of PLEs at the grid scale are shown in Fig. 3 and Table 3. On the whole, the functional value of Production Space (PS), Living Space (LS), and Ecological Space (ES) all exhibited an increasing trend across the Yanhe River Basin between 2000 and 2025, with a clear shift toward concentration in high–value zones. Spatially, the high–value zone of LS demonstrated a noticeable degree of spatial agglomeration, primarily concentrated along the main stream of the Yanhe River. In contrast, the functional value of PS and ES were more spatially dispersed throughout the basin.

Table 3
The area proportions of diverse categories for PLEs in Yanhe River Basin from 2000 to 2025

Functions	Year	Area proportions		
		High–value zone	Moderate–value zone	Low–value zone
PS	2000	44.90%	43.10%	12.00%
	2020	53.00%	31.60%	15.30%
LS	2000	0.10%	0.20%	99.70%
	2020	0.10%	0.40%	99.50%
ES	2000	55.80%	42.80%	1.40%
	2020	67.30%	31.30%	1.40%

In terms of the change in PS, its functional value exhibited an upward trend at the grid scale from 2000 to 2025. The high–value zone expanded from 44.9% to 53.0%, while the moderate–value zone declined from 43.1% to 31.6% and the low–value zone increased from 12.0% to 15.3%, indicating a shift toward higher production value categories across the basin. The functional value of LS increased modestly, with high–value zones concentrated in the Baota District, rising from 0.1% to 0.1%. The moderate–value LS zone expanded from 0.2% to 0.4%. The vast majority remained low–value (99.7% and 99.5%). The functional value of ES showed a substantial upward trend. The high–value zone expanded from 55.8% to 67.3%, becoming the dominant category, while the moderate–value zone declined from 42.8% to 31.3%. The low–value zone remained at approximately 1.4%, nearly disappearing across the basin. This improvement was most pronounced in the southeastern and northwestern parts

3.2 Multidimensional gradient differentiation of PLEs

3.2.1 Natural gradient differentiation of PLEs

(1) Terrain gradient differentiation of PLEs

The area coverage, mean functional value, and pixel–level change patterns of PLEs across five slope classes are presented in Fig. 4. The steepest slope category (> 25°) dominated the basin, accounting for

approximately 95% of the total area. Pixel–level analysis revealed that the most dramatic PLE transformations occurred in slope class I (< 3°), where 44.88% of PS pixels and 45.70% of ES pixels experienced functional value increases, with mean values surging by + 55.1% (PS, from 2.07 to 3.21) and + 69.5% (ES, from 2.21 to 3.74), reflecting large–scale Grain for Green implementation and urban expansion in flat terrain. In moderate slopes (II–III, 3–15°), PS increases were more moderate (10–15% pixels increased), while ES exhibited a mixed pattern with 6–7% pixel increases but 15–22% decreases, resulting in net mean ES declines of − 17.7% and − 8.8%, respectively. In steep slopes (IV–V, > 15°), ES pixel increases rose to 10–17% and mean ES increased by + 5.9% in the steepest category. LS changes were minimal across all slope classes, with the largest pixel increase rate being 8.92% in class II, though the mean LS still grew by + 97.5% in that zone due to the low baseline value. Slope class I occupied about 0.50% of the basin area.

Driving mechanism analysis: The terrain gradient analysis reveals that slope constraints significantly modulate the effectiveness of land use policies. In flat terrain (Class I), the high PS and ES gains are attributable to two converging drivers: (1) large–scale afforestation and grassland restoration under the Grain for Green Program, which preferentially targets accessible flat lands for agricultural abandonment; and (2) urban expansion, which preferentially occurs on level ground due to lower construction costs. In steep terrain (Classes IV–V), the ES gains (+ 5.9% in Class V) provide empirical evidence that ecological restoration programs can effectively penetrate marginal lands, contrary to conventional assumptions about terrain–limited policy implementation. The ES declines in moderate slopes (II–III) likely reflect the residual effects of livestock grazing and incomplete vegetation recovery in transition zones where restoration policies have been partially implemented.

(2) Elevation gradient differentiation of PLEs

The area coverage, mean functional value, and pixel–level change patterns of PLEs across five elevation ranges are presented in Fig. 4. The most dramatic PLE transformations occurred in the lowest elevation zone (< 945 m), which accounts for approximately 7.39% of the basin area. In this zone, 13.71% of PS pixels and 15.53% of ES pixels increased in functional value, with mean PS surging by + 3.3% (from 3.80 to 3.93) and mean ES increasing by + 5.0% (from 4.20 to 4.40). Middle and high elevation zones (II–V, > 945 m) exhibited more moderate changes: PS pixel increases ranged from 14.21% to 15.56%, ES pixel increases from 16.27% to 17.92%, and ES pixel decreases from 5.20% to 6.13%. Correspondingly, mean PS increased modestly (+ 2.5% to + 3.2%) and mean ES rose by + 4.2% to + 7.1% across these zones. LS changes were negligible across all elevations, with pixel increase rates below 1% in all classes.

Driving mechanism analysis: The elevation gradient pattern can be interpreted through the lens of human settlement patterns and agricultural land use traditions. Low elevation zones (< 945 m) serve as the primary corridors for human activities and transportation networks, where urbanization drives concentrated land use intensification. The PS and ES improvements in low elevation zones reflect agricultural intensification and successful vegetation restoration in valley floors. The relatively uniform PS and ES pixel increase rates across middle and high elevation zones (II–V) suggest that ecological

restoration policies have been implemented with comparable intensity across elevation bands, likely due to the basin–oriented management approach that does not strictly differentiate by elevation. The consistent elevation–driven gradient in PLE changes underscores the continuing primacy of topographic accessibility in shaping land use outcomes in the Loess Hilly–Gully region.

(3) River gradient differentiation of PLEs

Proximity to rivers plays a critical role in determining the accessibility and utilization efficiency of water resources. The area coverage, mean functional value, and pixel–level change patterns of PLEs across five river–distance classes are presented in Fig. 4. The vast majority of the Yanhe River Basin (83.07%) is located more than 1200 m from rivers, where the most significant pixel–level changes were observed: 14.85% of PS pixels and 16.97% of ES pixels increased in functional value, with mean PS rising by + 2.9% (from 3.69 to 3.80) and mean ES increasing by + 5.7% (from 4.09 to 4.32). In near–river zones (I–IV, < 1200 m), PS pixel increase rates were relatively uniform at 14–15%, with mean PS gains of + 1.8% to + 2.2%. ES pixel increases ranged from 15.42% to 18.31% in near–river zones, with mean ES gains of + 4.2% to + 6.2%. LS changes were modest across all river zones, with pixel increase rates below 1% and mean LS gains of + 40.3% to + 67.6% due to the low baseline. Overall, the river gradient showed a relatively balanced distribution of PLE changes compared to terrain gradients, with the most pronounced ecological improvement concentrated in the remote areas farthest from river channels.

Driving mechanism analysis: The river proximity gradient reveals a counter–intuitive pattern where the most pronounced ecological improvements occurred in remote areas far from rivers (Class V, > 1200 m). This pattern can be attributed to the top–down policy implementation of the Grain for Green Program, which explicitly prioritized remote, sloping, and ecologically degraded lands for restoration. These remote zones, previously excluded from intensive agricultural use due to water accessibility constraints, became primary targets for afforestation and grassland restoration. In contrast, near–river zones experienced more moderate ES gains, likely because these areas were already under some form of ecological protection or were less targeted by restoration programs due to their potential for agricultural or residential use. The balanced distribution of PLE changes across the river gradient suggests that water accessibility, while important for traditional land use, has been superseded by policy–driven land use planning in shaping the ecological trajectory of the basin.

3.2.2 Socio–economic gradient differentiation in PLEs

(1) Population gradient differentiation in PLEs

The area coverage, mean functional value, and pixel–level change patterns of PLEs across five population density categories are presented in Fig. 5. It is important to note that the 2000 and 2025 population data originate from different WorldPop versions with distinct resolution characteristics, making direct area comparisons across years unreliable. In the highest population density zone (I, > 22 p/km²), 15.57% of PS pixels and 14.56% of LS pixels increased, with mean PS rising by + 11.7% and mean LS increasing by + 35.0%. However, 26.52% of ES pixels decreased, leading to a mean ES decline

of − 36.7% (from 3.22 to 2.04), indicating that construction activities in high–density areas encroached on ecological space. In the sparsest zone (V, < 1.3 p/km²), which accounts for 15.66% of the 2025 basin area, 10.98% of PS pixels and 11.72% of ES pixels increased, while mean PS slightly declined by − 1.2%, reflecting the reclassification effect of the updated population data. LS showed notable mean value gains across zones III–V (+ 95.9% to + 719.1%) despite low pixel increase rates, due to very low baseline LS values in sparsely populated areas.

Driving mechanism analysis: The population density gradient reveals a fundamental tension between urbanization and ecological maintenance. In high–density zones (Class I), the PS and LS gains (+ 11.7% and + 35.0%, respectively) combined with a sharp ES decline (–36.7%) indicate a classic urbanization–driven land use conversion pattern, where urban expansion consumes adjacent ecological space to meet residential and commercial demand. This pattern reflects the concentrated development model that prioritizes economic efficiency over ecological conservation in areas with high population pressure. In sparsely populated zones (Class V), the ES improvements (+ 11.72% pixel increase) can be attributed to the effective implementation of the Grain for Green Program in areas where human interference is minimal, allowing vegetation to recover with limited disturbance. The pronounced LS gains in zones III–V (+ 95.9% to + 719.1%) are partly attributable to rural infrastructure development and village consolidation, which raise baseline LS values in previously underserved areas. These contrasting patterns underscore the dual influence of population pressure as both a driver of ecological degradation in urban cores and a precondition for ecological recovery in rural margins.

(2) Economic gradient differentiation in PLEs

Nighttime light intensity is widely recognized as an indicator of regional economic development. The area coverage, mean functional value, and pixel–level change patterns of PLEs across five nightlight intensity classes are presented in Fig. 5. It must be noted that the 2000 data (DMSP/OLS, 1000 m resolution) and 2025 data (VIIRS–based, 500 m resolution) are from fundamentally different sensors, and therefore area coverage comparisons across years are not directly interpretable. In the highest nightlight zone (I, > 20 DN), which accounted for 3.18% of the basin area in 2000, 26.05% of PS pixels and 12.05% of LS pixels increased, while 47.27% of ES pixels decreased——the highest ES decrease rate among all gradient classes. Correspondingly, mean PS increased by + 34.8% (from 2.90 to 3.91) and mean LS by + 648.1% (from 0.125 to 0.933), while mean ES declined by − 47.5% (from 3.32 to 1.74) due to urban expansion encroaching on ecological space. In low nightlight zones (IV–V, < 6 DN), which dominated the 2025 landscape (97.33% of area), PS pixel increases ranged from 14.33% to 14.04%, ES pixel increases from 16.16% to 16.54%, with mean ES gains of + 1.5% to + 5.3%. The contrasting patterns between high and low nightlight zones reflect the urban–rural dichotomy: urban core expansion drove PS and LS growth at the expense of ES, while the vast rural matrix experienced broad–based ecological improvement.

Driving mechanism analysis: The nighttime light gradient provides a spatial proxy for economic development intensity and reveals pronounced urban–rural functional trade–offs. In high nightlight

zones (Class I), the dramatic ES decline (–47.5%) coupled with strong PS and LS gains (+ 34.8% and + 648.1%) constitutes the most significant land use conflict identified in this study. This pattern reflects the development–led land conversion model, where economic growth drives direct encroachment on ecological space through construction of residential, commercial, and industrial facilities. The 97.33% of basin area in low nightlight zones (Classes IV–V) that exhibited consistent ES improvements (+ 1.5% to + 5.3%) represent the rural matrix where the Grain for Green Program has been the dominant driver of landscape change. The stark ES differential between urban cores (–47.5%) and rural margins (+ 1.5% to + 5.3%) raises concerns about net basin–level ecosystem service balances, suggesting that ES gains in rural areas may not fully compensate for ES losses in urban cores due to differences in ecological quality and service capacity.

(3) Transportation gradient differentiation in PLEs

The area coverage, mean functional value, and pixel–level change patterns of PLEs across five road accessibility classes are presented in Fig. 5. The road network expansion over this period was substantial, with the near–road zone (< 500 m) expanding from 19.19% to 25.09% (+ 5.90 percentage points) and the remote zone (> 6000 m) contracting from 8.82% to 4.58% (–4.24 percentage points). Pixel–level analysis revealed a clear gradient effect: as distance from roads increased, the proportion of pixels with PS and ES functional value increases exhibited a non–monotonic pattern (PS: 13.88% in class I to 15.09% in class III then 13.88% in class V; ES: 15.31% in class I to 18.55% in class II then 15.56% in class V). Correspondingly, mean PS gains increased from + 3.0% (class I) to + 4.9% (class IV), and mean ES gains rose from + 3.8% (class I) to + 8.9% (class V). The most striking pattern was in the remote zone (> 6000 m), where ES mean value grew from 4.14 to 4.51 (+ 0.37 absolute, + 8.9%), representing substantial ecological improvement in previously inaccessible areas. LS changes were negligible across all road zones, with pixel increase rates below 1%. The consistent gradient pattern——gains increasing with distance from roads——indicates a spatial convergence of PLE functional values as remote areas previously limited by poor accessibility experienced the most dramatic ecological and agricultural improvements.

Driving mechanism analysis: The transportation gradient reveals a dual–role mechanism of infrastructure expansion in shaping PLE spatial patterns. First, near–road zones (Class I) experienced PS and ES gains (+ 3.0% and + 3.8%) due to agricultural intensification and afforestation along transport corridors, which improve market access for agricultural products and reduce the cost of transporting seedlings and materials for restoration projects. Second, and more counterintuitively, the most dramatic ES improvements (+ 8.9%) occurred in the most remote zones (Class V, > 6000 m), where road access was previously minimal. This pattern can be explained by the indirect governance effect of infrastructure development: as road networks expand and penetrate previously inaccessible areas, project managers, monitoring teams, and technical experts gain improved access to remote restoration sites, enabling more effective implementation, monitoring, and adaptive management of ecological restoration programs. The spatial convergence of PLE functional values——where remote areas "catch up" with accessible areas——suggests that infrastructure development has facilitated the spatial equalization of

ecological outcomes, rather than exacerbating spatial inequalities as conventional wisdom might suggest.

4 Discussions

4.1 The overall functional changes in PLEs during 2000–2025

The findings of this study indicated that over the 25 years from 2000 to 2025, the overall functional value of LS and ES increased, while that of PS experienced fluctuations. In terms of the overall functional changes of PLEs, the total area of PS in the Yanhe River Basin was the greatest, accounting for more than 60% of the total area, demonstrating a declining trend in both area coverage and functional value. This decline in PS can be attributed to two factors: the continuous conversion of arable land to forest and grassland driven by the Grain for Green program, and the conversion of arable land to built–up areas resulting from urbanization. The functional value of LS increased overall, despite the proportion of high–value areas (concentrated in the Baota District) being relatively small. This improvement of LS was supported by the significant expansion in both the high–value zone areas and overall functional value. The functional value and area coverage of ES increased significantly, reflecting the success of ecological restoration efforts in the region.

The gradient–level analysis of PLEs allowed for a spatially explicit characterization of landscape functional dynamics, where both natural and socio–economic constraints played pivotal roles. The spatially explicit PLE gradient analysis revealed that the most significant spatial restructuring of landscape functions occurred in the slope range of less than 25 degrees, elevations below 1100 m, and areas within 1200 m of river channels. The results suggested that spatial differentiation of production and living functions is primarily governed by the intensity of human activities which exhibit a clear gradient from the valley floor to the ridge top. The areas with moderate population density (3–22 persons/km²) provided a trade–off point in PLE reconfiguration, with ecological space improvements being most pronounced in these regions.

4.2 Critical analysis of PLEs theory: contributions and challenges

This study contributes to the theoretical advancement of PLEs research in several critical dimensions. First, by operationalizing the abstract PLE concept through a grid–scale functional value scoring system, this research bridges the gap between theoretical land use classification and quantitative spatial assessment. The proposed scoring framework (PS: 0–5, LS: 0–5, ES: 0–5) offers a replicable methodology for measuring the multi–functional characteristics of land use in comparable basins worldwide. Second, the integration of six gradient dimensions (slope, elevation, river proximity, population density, nighttime light, and road accessibility) provides a holistic perspective on PLE spatial differentiation that transcends conventional single–factor analyses. This multidimensional gradient

approach enables a more nuanced understanding of how natural topography and human activities jointly shape PLE patterns. Third, the pixel–level change detection methodology employed in this study represents a methodological contribution, as it captures heterogeneous transformations within gradient classes that are often masked by aggregate statistical summaries.

Nevertheless, several theoretical challenges merit critical attention. The PLE framework, while conceptually intuitive, faces inherent limitations when applied to complex landscape mosaics where multiple functions coexist in a single land parcel. Our discrete scoring approach, which assigns dominant functional scores based on land use type, may oversimplify the multi–functionality of land systems, particularly in transitional zones where production, living, and ecological functions are intimately intertwined (Zhang et al., 2026). Additionally, the assumption of spatial independence among gradient factors may not fully capture their synergistic or antagonistic interactions. For instance, the combined effect of road expansion and terrain accessibility on PLE restructuring likely involves complex non–linear feedbacks that cannot be adequately represented by marginal gradient analyses alone. Future research should explore spatially explicit interaction terms or geographically weighted regression models to better account for these co–dependent relationships.

4.3 Driving mechanism analysis of PLEs transformation

The observed PLE transformations in the Yanhe River Basin can be attributed to the intertwined effects of top–down policy interventions and bottom–up socioeconomic dynamics. The most significant driver of ES improvement and PS restructuring is the Grain for Green Program, which has been implemented systematically since 1999 across the Loess Plateau. Our gradient analysis revealed that ES gains were most pronounced in steep slope areas (Class V, > 25°) and remote regions (distance from river > 1200 m), precisely the zones targeted by afforestation and grassland restoration policies. This spatial pattern provides empirical evidence that large–scale ecological restoration programs can effectively reach remote and topographically challenging terrain, contrary to conventional assumptions about limited policy implementation capacity in marginal lands.

Urbanization constitutes the second major driving force, primarily affecting the LS dimension and exerting indirect effects on PS and ES through land use conversion. The concentration of LS high–value zones along the main course of the Yanhe River and in the Baota District reflects the spatially clustered nature of urban development, which tends to follow existing infrastructure corridors and favorable terrain. The gradient analysis of nighttime light intensity revealed a stark urban–rural dichotomy: high nightlight zones (Class I, > 20 DN) experienced substantial ES declines (–47.5% mean change) due to construction encroachment, while the vast rural matrix (97.33% of basin area, Classes IV–V) showed consistent ES improvements (+ 1.5% to + 5.3%). This contrast highlights the environmental trade–offs inherent in urbanization, where economic development in concentrated areas may come at the expense of ecological space in high–intensity development zones.

Infrastructure expansion, particularly road network development, emerges as a third critical driver that modulates the spatial accessibility of previously remote areas. The expansion of near–road zones (Class

I, < 500 m) by 5.90 percentage points indicates substantial infrastructure investment that has shortened travel times and improved market access across the basin. Counterintuitively, the most dramatic ES improvements occurred in remote zones (Class V, > 6000 m), where mean ES increased by + 8.9%. This pattern suggests that infrastructure development may have facilitated the implementation of ecological restoration programs in areas previously inaccessible to project managers and monitoring teams, rather than triggering immediate land use intensification in these zones.

4.4 Recommendations for future research methodologies

To deepen the mechanistic understanding of PLE transformation and enhance the predictive capability of land use planning, future research should consider integrating multiple methodological approaches. First, questionnaire surveys and field interviews with local land managers, farmers, and policymakers would provide valuable insights into the decision–making processes underlying land use conversions at the household and community scales. Such qualitative data could help validate the statistical associations identified in this study and uncover micro–level drivers that are not captured by remote sensing or census data. Second, econometric modeling techniques, such as panel data regression, spatial Durbin models, or geographically weighted regression (GWR), could be employed to quantify the relative contributions of different drivers and test for spatial non–stationarity in driver–response relationships. Third, scenario simulation approaches, including land use transformation (LUT) models and cellular automata (CA) integrated with multi–agent systems (MAS), could be used to project future PLE configurations under alternative policy pathways, thereby informing adaptive management strategies. The methodological integration of remote sensing quantification, statistical modeling, qualitative investigation, and scenario simulation would constitute a comprehensive analytical framework that advances PLE research from descriptive diagnosis toward predictive planning (Wang et al., 2016).

4.5 Policy implications

The results of this study provide important insights for future land use planning, ecological management and rural revitalization in the Loess Hilly–Gully region. First, the gradient–level analysis highlights the need for spatially differentiated management strategies to support rural development. The highest concentration of PLE changes and potential land use conflicts was observed in the slope range of 0–3 degrees, a critical zone for agricultural land preservation, urban expansion and rural construction. Therefore, it is recommended that agricultural land be strictly protected while maintaining a balance between economic development, ecological conservation and rural revitalization in gentler sloping areas. Second, the significant expansion in the functional value of ES across both the most sparsely and densely populated areas suggests that a dual–activating mechanism for ecological improvement has emerged in the basin, which also underpins rural revitalization. In sparsely populated areas, ecological gains should be sustained through continued implementation of the Grain for Green program to boost rural development, while in densely populated urban areas, urban green space planning should be enhanced to improve local ecological service provision and advance urban–rural coordinated revitalization. Third, given the dominant role of road network expansion in PLE spatial restructuring,

future infrastructure planning should incorporate anticipatory ecological impact assessments to avoid compromising ecological gains achieved in remote areas and hinder local rural revitalization (Zhao et al., 2015).

5 Conclusions

This study systematically analyzed the multi–dimensional gradient differentiation of PLEs in the Yanhe River Basin from 2000 to 2025 by constructing a grid–scale functional value evaluation system. Unlike conventional PLE studies that rely on land use type classification or administrative–unit statistics, this research operationalized the PLE framework at the pixel level and examined how natural and socio–economic gradients jointly shape the spatial restructuring of landscape functions. The unique patterns and scientific insights emerging from this analysis are summarized as follows.

(1) Unique pattern of ES–led functional intensification in remote terrain. Contrary to the conventional expectation that ecological improvements concentrate in accessible, low–elevation zones, this study revealed that the most dramatic ES gains occurred in the steepest slope zones (> 25°, mean ES + 5.9%) and the most remote river–distance zones (> 1200 m, mean ES + 5.7%). This counterintuitive pattern provides empirical evidence that large–scale ecological restoration policies, particularly the Grain for Green Program, can effectively reach and transform marginal lands that were previously inaccessible. The finding challenges the assumption that terrain constraints fundamentally limit the spatial reach of land use management interventions.

(2) Asymmetric urban–rural PLE trajectories along economic gradients. The nighttime light gradient analysis revealed a stark spatial dichotomy: high–development zones experienced substantial PS and LS gains at the direct expense of ES (mean ES decline of − 47.5% in the highest nightlight zone), while the vast rural matrix (97.33% of basin area) exhibited consistent multi–dimensional improvements (+ 1.5% to + 5.3% ES gains). This asymmetric trajectory indicates that urbanization in the Yanhe River Basin follows a concentrated development model that prioritizes local functional intensification over distributed ecological maintenance. The gradient–level evidence suggests that ES losses in urban cores may not be fully compensated by rural ecological gains, raising concerns about net basin–level ecosystem service balances.

(3) Infrastructure–mediated spatial convergence of PLE functional values. The expansion of near–road zones by 5.90 percentage points, coupled with the most pronounced ES improvements in the most remote zones (Class V, > 6000 m, mean ES + 8.9%), suggests that road infrastructure development facilitated rather than hindered ecological restoration in inaccessible areas. This finding implies a convergence mechanism where improved accessibility enables policy implementation, monitoring, and adaptive management in previously marginalized zones. The spatial redistribution of PLE functional values thus reflects not only direct land use changes but also the indirect effects of infrastructure on governance capacity.

In conclusion, this study contributes to the theoretical understanding of PLE spatial reorganization by demonstrating the primacy of policy–driven ecological restoration over terrain constraints, the asymmetric urbanization–ecology trade–off across economic gradients, and the infrastructure–mediated convergence of landscape functions in remote areas. These unique patterns provide a scientific basis for differentiating PLE management strategies in the Loess Hilly–Gully region: ecological maintenance programs should be sustained and expanded in remote steep terrain, urban green infrastructure planning should be strengthened to offset ES losses in high–development zones, and infrastructure planning should incorporate anticipatory ecological impact assessments to preserve gains achieved in previously inaccessible areas. The multi–dimensional gradient methodology developed in this study offers a transferable analytical framework for diagnosing PLE spatial reorganization in comparable mountainous basins worldwide.

Declarations

Ethical Approval

Not applicable.

Funding

This work was supported by the Major Program of National Natural Science Foundation of China (No. 42293270), National Natural Science Foundation of China (No. 42271279), Guizhou Provincial Youth Guiding Fund Project (Grant No. [2025]012) and Guizhou University Talent Introduction Scientific Research Project (600429243301).

Author Contribution

Z.X. performed data collection and data analysis, and wrote the original manuscript. W.H.T. participated in data sorting and manuscript revision. C.Z. supervised the study, reviewed and revised the manuscript. All authors have read and approved the final manuscript.

Acknowledgement

This work was supported by the Major Program of National Natural Science Foundation of China（No. 42293270）, National Natural Science Foundation of China (No. 42271279), Guizhou Provincial Youth Guiding Fund Project (Grant No.[2025]012) and Guizhou University Talent Introduction Scientific Research Project (600429243301).

Availability of data and materials

The raw datasets generated and analysed in this study are not publicly available due to relevant restrictions.

References

1. Bondarenko, I., Kokhan, N., Gonchar, O., Bondarenko, B., 2020. Man–made landforms in landscape design of territories as a means of solving environmental problems. *Architecture, Civil Engineering, Environment*, 13(4). doi: 10.21307/ACEE-2019-047.
2. Hu, Q., Zhang, Z., Niu, L., 2022. Identification and evolution of territorial space from the perspective of composite functions. *Habitat International*, 128(000):15. doi: 10.1016/j.habitatint.2022.102662.
3. Winkler, K., Fuchs, R., Rounsevell, M., Herold, M., 2021. Global land use changes are four times greater than previously estimated. *Nature Communications*, 12:2501. doi: 10.1038/s41467-021-22702-2.
4. Trindade Rodrigues, M. T., Silva Júnior, J. A., Ferreira Filho, H. R., 2026. Land use and land cover changes in Conceição do Araguaia. *Environmental & Social Management Journal*, 20(1). doi: 10.24857/rgsa.v20n1-004
5. Verburg, P. H., van de Steeg, J., Veldkamp, A., Willemen, L., 2009. From land cover change to land function dynamics: A major challenge to improve land characterization. *Journal of Environmental Management*, 90(3):1327–1335. doi: 10.1016/j.jenvman.2008.08.005.
6. Liu, J., Liu, Y., Li, Y., 2017. Classification evaluation and spatial–temporal analysis of "production–living–ecological" spaces in China. *Acta Geographica Sinica*, 72(7):1290–1304. doi: 10.11821/dlxb201707013
7. Ji, Z., Liu, C., Xu, Y., Sun, M., Wei, H., Sun, D., 2023. Quantitative identification and the evolution characteristics of production–living–ecological space in the mountainous area: From the perspective of multifunctional land. *Journal of Geographical Sciences*, 33(4):779–800. doi: 10.1007/s11442-023-2106-x.
8. Gao, C., Li, S., Bao, H., Zhang, Y., 2025. Multi–dimensional driving mechanisms and scenario simulation of production–living–ecological space evolution in urban agglomerations of china: evidence from the guanzhong plain. *Land*, 14(11). doi: 10.3390/land14112201.
9. Lin, G., Jiang, D., Fu, J., 2022. A review on the overall optimization of production–living–ecological space: Theoretical basis and conceptual framework. *Land*, 11(3):345. doi: 10.3390/land11030345.
10. Liu, Z., Huang, J., Liu, X., 2025. Construction and analysis of the ecological security pattern in territorial space in Shaanxi of the Yellow River basin, China. *Atmosphere*, 16(2):217. doi: 10.3390/atmos16020217
11. Philpott, S. M., Lin, B. B., Jha, S., 2008. A multi–scale assessment of hurricane impacts on agricultural landscapes based on land use and topographic features. *Agriculture, Ecosystems & Environment*, 128(1–2):12–20. doi: 10.1016/j.agee.2008.04.016.

12. Liao, G., He, P., Gao, X., Lin, Z., Huang, C., Zhou, W., 2022. Land use optimization of rural production–living–ecological space at different scales based on the BP–ANN and CLUE–S models. *Ecological Indicators*, 137:108710. doi: 10.1016/j.ecolind.2022.108710.
13. Yu, S. H., Deng, W., Xu, Y. X., Zhang, X., Xiang, H. L., 2020. Evaluation of the production–living–ecology space function suitability of Pingshan County in the Taihang mountainous area, China. *Journal of Mountain Science*, 17(10):2562–2576. doi: 10.1007/s11629-019-5776-1.
14. Valdivia–Orrego, O., Peña–Cortés, F., 2024. Mountain territories: The need to approach territorial planning and governance. *Planning Theory & Practice*, 25(5):731–740. doi: 10.1080/14649357.2024.2444779.
15. Chen, Y., Zhu, M., 2022. Spatiotemporal evolution and driving mechanism of "production–living–ecology" functions in China: a case of both sides of hu line. *International Journal of Environmental Research and Public Health*, 19(6):3488. doi: 10.3390/ijerph19063488.
16. Uhodnikova, O., Rudachenko, O., Troian, V., 2024. Evaluation and analysis of the socio–economic potential of territorial communities. *Multidisciplinary Science Journal*, 7(1):2025006. doi: 10.31893/multiscience.2025006.
17. Li, S., Zhu, C., Deng, X., 2024. Exploring the urban–rural gradient effects of construction land expansion processes on land use function trade-off/synergy in rapidly urbanizing areas. *Land Degradation and Development*, 35(1):1. doi: 10.1002/ldr.4896.
18. Tao, J., Lu, Y., Ge, D., 2022. The spatial pattern of agricultural ecosystem services from the production–living–ecology perspective: A case study of the Huaihai Economic Zone, China. *Land Use Policy*, 122:106355. doi: 10.1016/j.landusepol.2022.106355.
19. Liu, Y. Q., Tan, X., Duan, G. L., 2025. Spatiotemporal dynamics and driving factors of soil organic carbon storage in the yangtze river basin under climate change and land use scenarios. *Soil Ecology Letters*, 7(4):250345. doi: 10.1007/s42832-025-0345-8.
20. Gu, C., Mu, X., Gao, P., 2019. Influence of vegetation restoration on soil physical properties in the Loess Plateau, China. *Journal of Soils and Sediments*, 19(2):716–728. doi: 10.1007/s11368-018-2083-3.
21. Schmitz, M. F., Matos, D. G. G., De Aranzabal, I., 2012. Effects of a protected area on land–use dynamics and socioeconomic development of local populations. *Biological Conservation*, 149(1):122–135. doi: 10.1016/j.biocon.2012.01.043.
22. Zhao, G., Li, E., Mu, X., 2015. Changing trends and regime shift of streamflow in the Yellow River basin. Stochastic Environmental Research & Risk Assessment, 29(5):1331–1343. doi: 10.1007/s00477-015-1058-9.
23. Wu, Y., Shi, K., Chen, Z., Liu, S., Chang, Z., 2021. An improved time–series DMSP–OLS–like data (1992–2024) in China by integrating DMSP–OLS and SNPP–VIIRS. *Harvard Dataverse*. doi: 10.7910/DVN/GIYGJU
24. Cai, Y., 2001. A study on land use/cover change: The need for a new integrated approach. *Geographical Research*, 6(20):645–652. doi: 10.11821/yj2001060001.

25. Wiggering, H., Dalchow, C., Glemnitz, M., 2006. Indicators for multifunctional land use—Linking socio–economic requirements with landscape potentials. *Ecological Indicators*, 6(1):238–249. doi: 10.1016/j.ecolind.2005.08.014.
26. Fu, J., Bu, Z., Jiang, D., 2022. Sustainable land use diagnosis based on the perspective of production–living–ecological spaces in China. *Land Use Policy*, 122:106386. doi: 10.1016/j.landusepol.2022.106386.
27. Groot, R. D., 2006. Function–analysis and valuation as a tool to assess land use conflicts in planning for sustainable, multi–functional landscapes. *Landscape & Urban Planning*, 75(3–4):175–186. doi: 10.1016/j.landurbplan.2005.02.016.
28. Zhang, X., Liu, K., Wang, S., Li, X., 2025. Ecological monitoring and service value assessment of river–lake shores: a case study of the huanggang and taihu segments of the yangtze river. *Land*, 14(5). doi: 10.3390/land14051038.
29. Ullah, S., Ahmad, K., Sajjad, R. U., 2019. Analysis and simulation of land cover changes and their impacts on land surface temperature in a lower Himalayan region. *Journal of Environmental Management*, 245:348–357. doi: 10.1016/j.jenvman.2019.05.063.
30. Li, Y., Song, R., Ren, P., 2025. A study on spatial and temporal changes and synergies/trade–offs of the production–living–ecological functions in mountainous areas based on the Niche Width Model. *Land*, 14(4):743. doi: 10.3390/land14040743
31. Fu, R., Wan, W., Qiao, L., 2026. Research on the evolution characteristics and interaction mechanism between socio–economy and the "production–living–ecological" functions of land use at the county level: a case study of henan province. *Land*, 15(3). doi: 10.3390/land15030459.
32. Cao, Z., Han, Z., Li, Y., 2024. Distribution of topographical changes triggered by prolonged heavy rainfall in the Chinese Loess Plateau: A case study of the Gutun catchment in Yan'an. *Journal of Geographical Sciences*, 34(3):571–590. doi: 10.1007/s11442-024-2218-y.
33. Chaif, H., Keyvanshokouhi, S., Finke, P., 2025. Introducing a volume change function in process–based modelling of soil development due to land management: A proof of concept. *Geoderma*, 455:117228. doi: 10.1016/j.geoderma.2025.117228.
34. Levin, N., Kyba, C. C. M., Zhang, Q., 2020. Remote sensing of night lights: A review and an outlook for the future. *Remote Sensing of Environment*, 237:111443. doi: 10.1016/j.rse.2019.111443.
35. Wondie, M., Teketay, D., Melesse, A. M., 2012. Relationship between topographic variables and land cover in the Simen Mountains National Park, a World Heritage Site in northern Ethiopia. *International Journal of Remote Sensing Applications*, 2(2):36–43. doi: 10.1155/2014/614249
36. Zhang, Z., Liu, Z., Yin, X., Zhang, H., Huang, F., 2026. Spatiotemporal evolution and drivers of production–living–ecological land in the northern Tianshan Mountains using complex network analysis. *Scientific Reports*, 16(1). doi: 10.1038/s41598-026-35910-x.
37. Wang, S., Fu, B., Piao, S., 2015. Reduced sediment transport in the Yellow River due to anthropogenic changes. *Nature Geoscience*, 9(1):38–41. doi: 10.1038/ngeo2602.

Figures

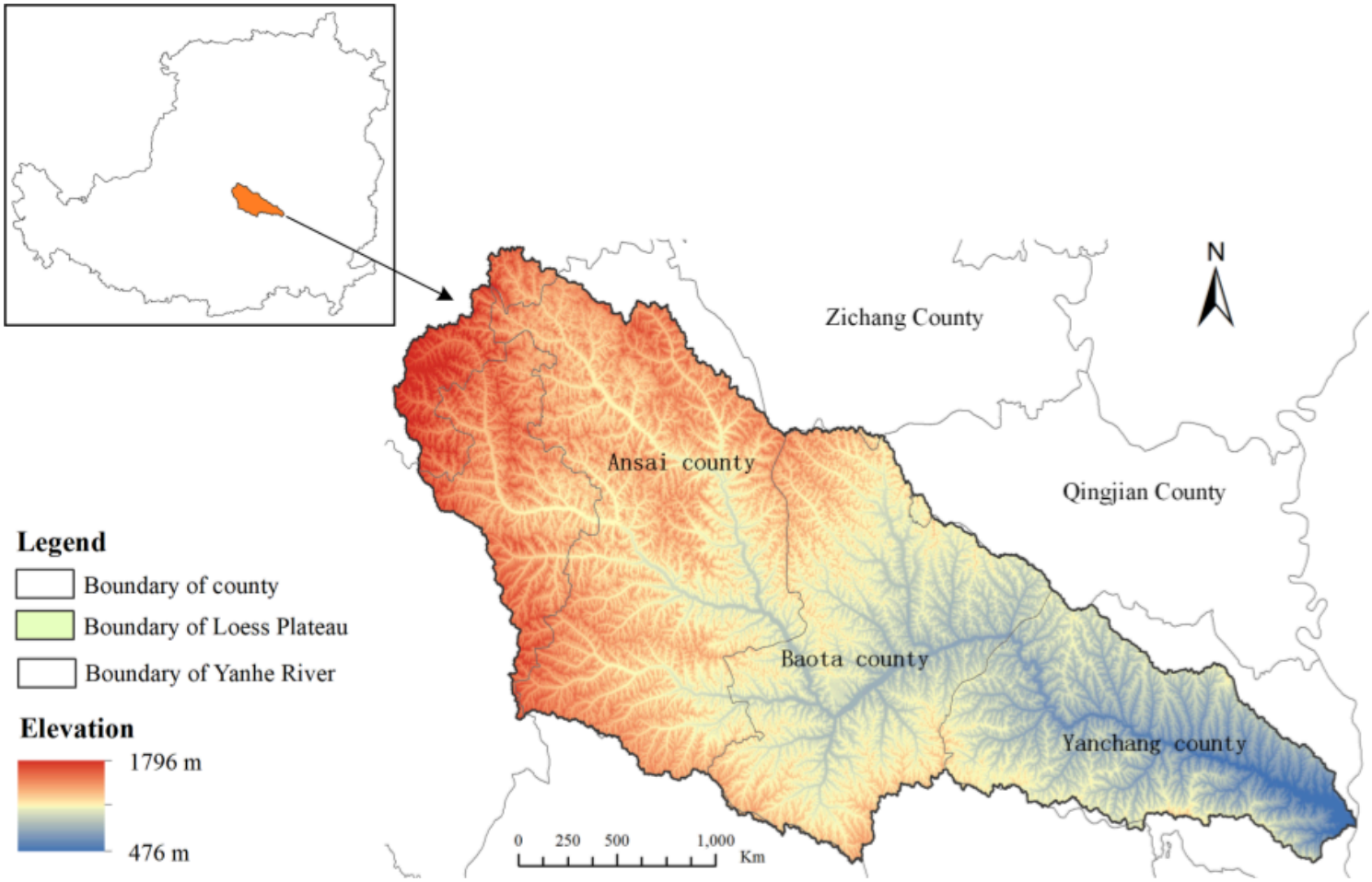


Figure 1

Location and elevation map of the study area

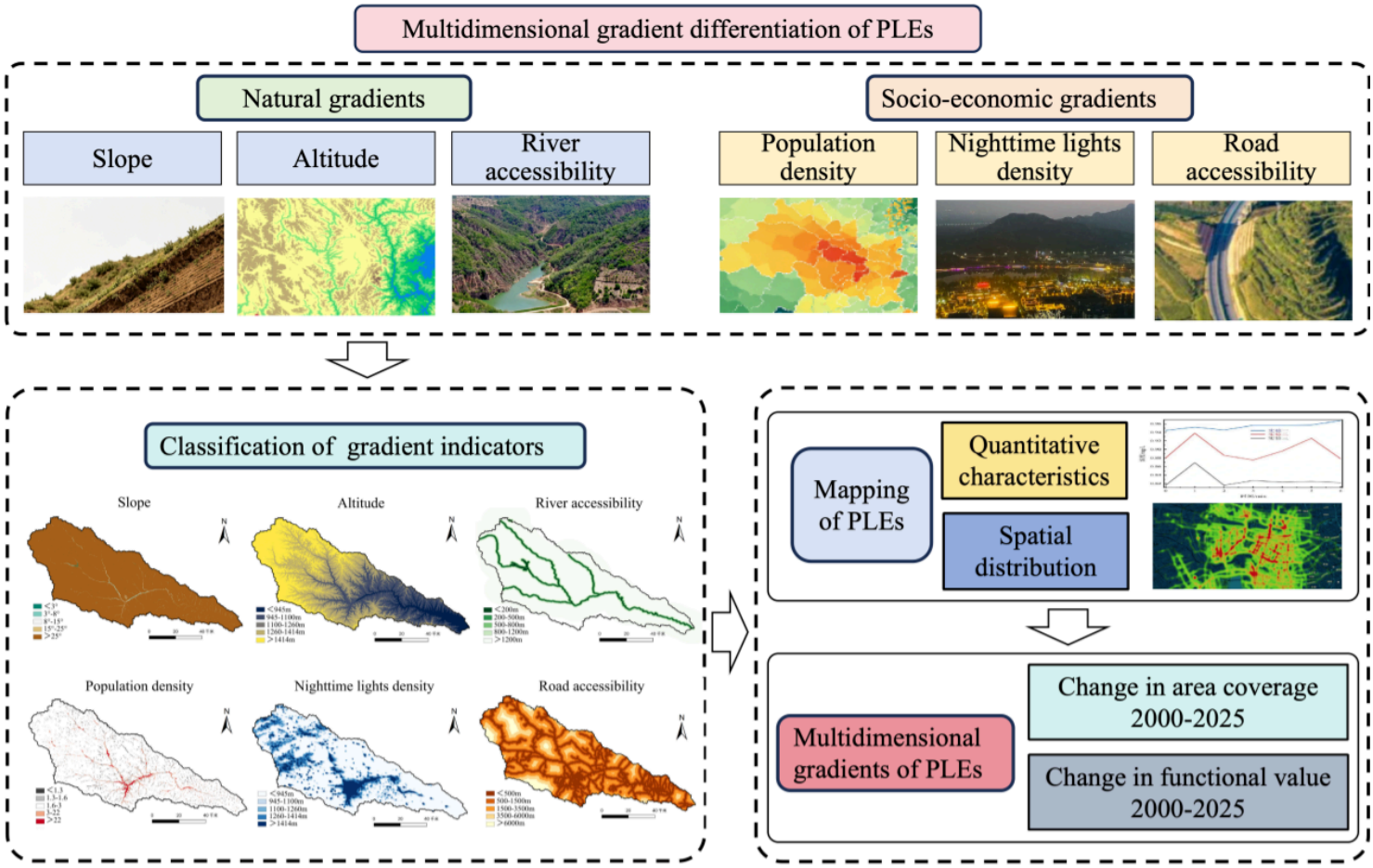


Figure 2

Framework of gradient differentiation for PLEs

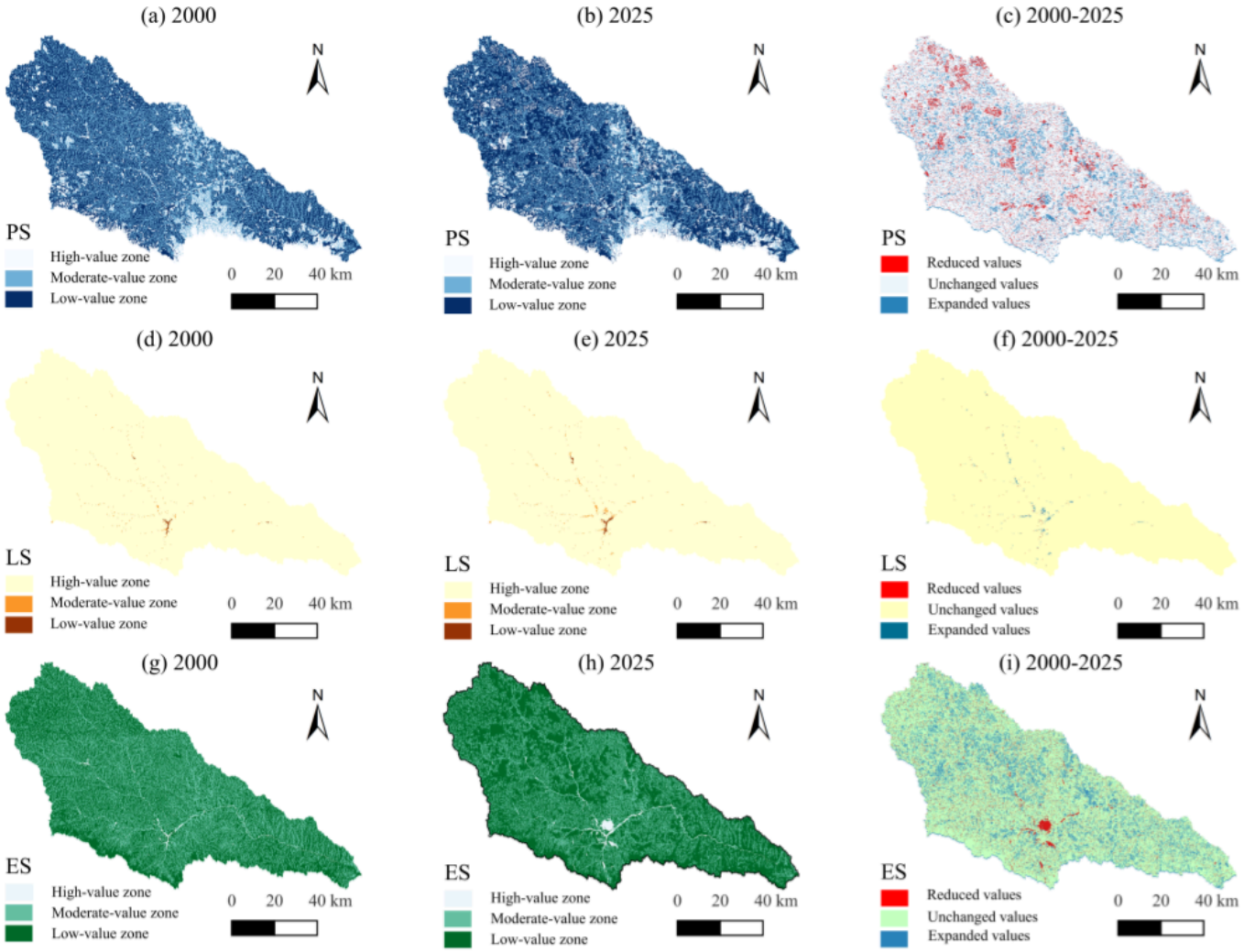


Figure 3

Spatial configuration and functional dynamics of PLEs in 2000 and 2025

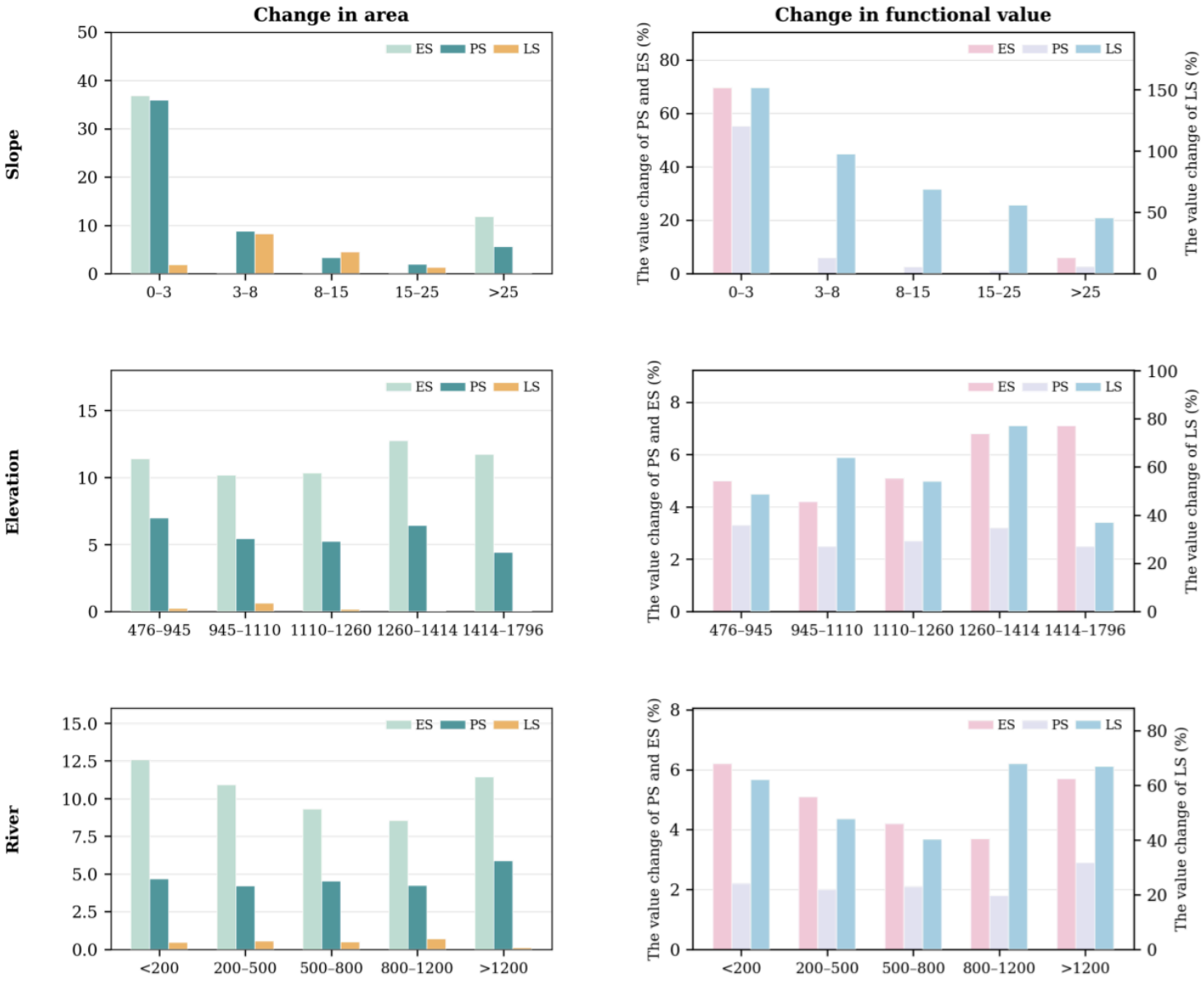


Figure 4

Natural gradient differentiation of PLEs during 2000–2025

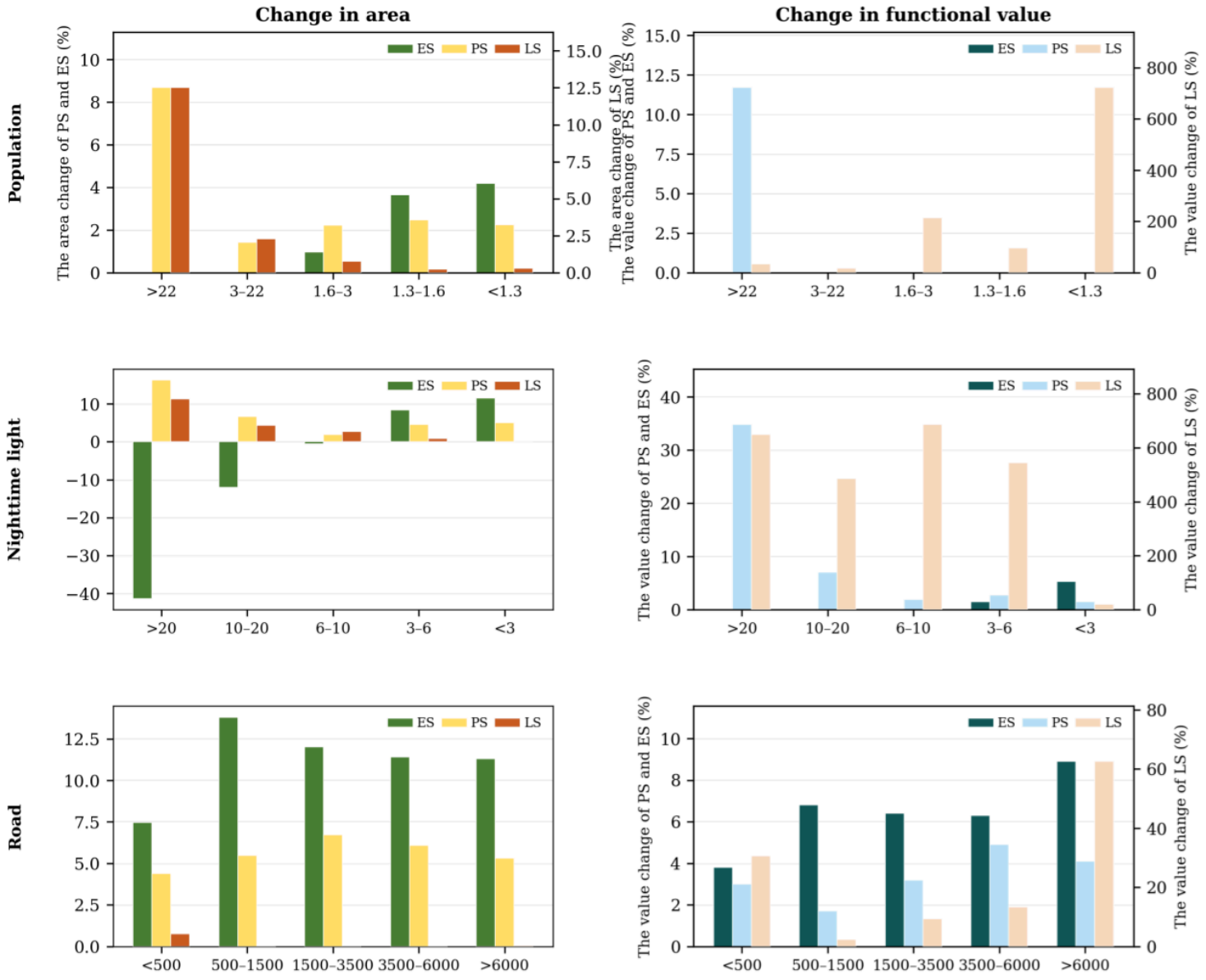


Figure 5

Socio–economic gradient differentiation of PLEs during 2000–2025